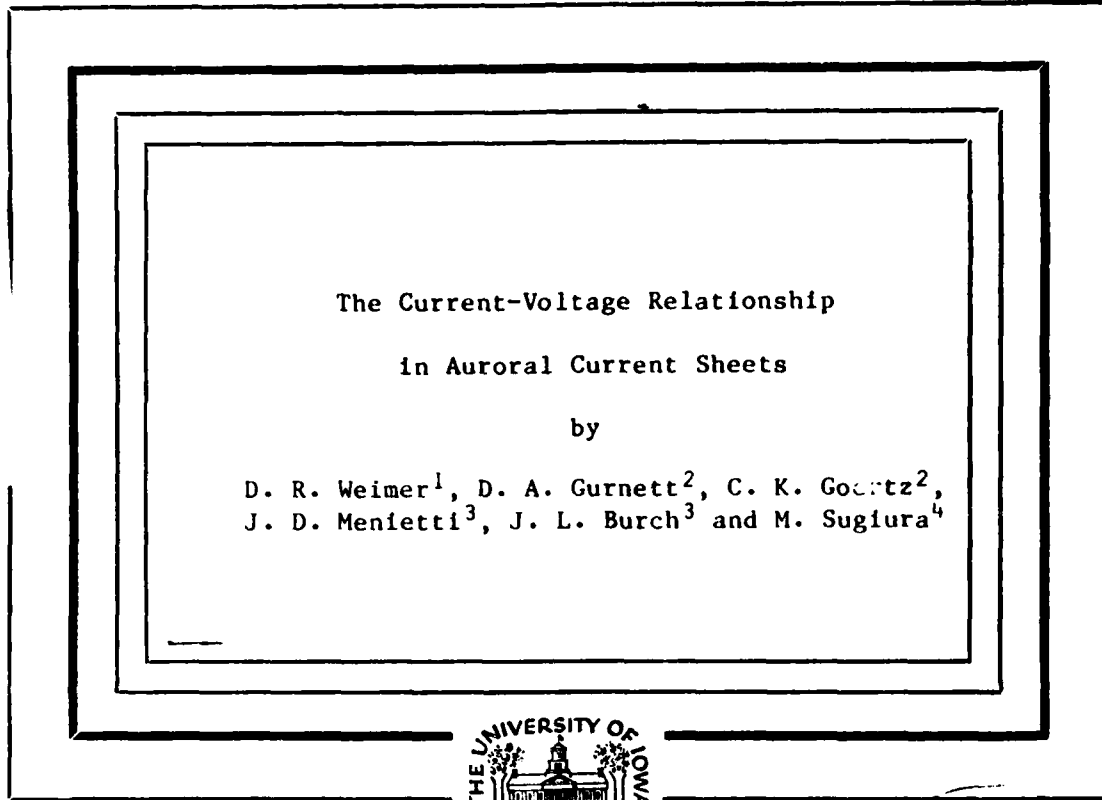


MICROCOPY

11701

12

AD-A169 074



DTIC
 ELECTE
 JUL 03 1986
 S D

DTIC FILE COPY

Department of Physics and Astronomy
THE UNIVERSITY OF IOWA

Iowa City, Iowa 52242

This document has been approved
 for public release and sale; its
 distribution is unlimited.

86 7 3 011

The Current-Voltage Relationship
in Auroral Current Sheets

by

D. R. Weimer¹, D. A. Gurnett², C. K. Goertz²,
J. D. Menietti³, J. L. Burch³ and M. Sugiura⁴

March 1986

Submitted to the J. Geophys. Res.

¹Regis College Research Center, 235 Wellesley St., Weston, MA 02193

²Physics and Astronomy, University of Iowa, Iowa City, IA 52242

³Southwest Research Institute, P.O. Drawer 28510, San Antonio, TX 78284

⁴Kyoto University, Kyoto, Japan

UNCLASSIFIED

SECURITY CLASSIFICATION OF THIS PAGE (When Data Entered)

REPORT DOCUMENTATION PAGE		READ INSTRUCTIONS BEFORE COMPLETING FORM
1. REPORT NUMBER U. of Iowa 86-21	2. GOVT ACCESSION NO. A169074	3. RECIPIENT'S CATALOG NUMBER
4. TITLE (and Subtitle) THE CURRENT-VOLTAGE RELATIONSHIP IN AURORAL CURRENT SHEETS	5. TYPE OF REPORT & PERIOD COVERED Progress 1986	
	6. PERFORMING ORG. REPORT NUMBER	
7. AUTHOR(s) D. R. WEIMER, D. A. GURNETT, C. K. GOERTZ, J. D. MENIETTI, J. L. BURCH and M. SUGIURA	8. CONTRACT OR GRANT NUMBER(s) N00014-85-K-0404	
9. PERFORMING ORGANIZATION NAME AND ADDRESS Dept. of Physics and Astronomy The University of Iowa Iowa City, IA 52242	10. PROGRAM ELEMENT, PROJECT, TASK AREA & WORK UNIT NUMBERS	
11. CONTROLLING OFFICE NAME AND ADDRESS Electronics Program Office Office of Naval Research Arlington, VA 22217	12. REPORT DATE March 1986	
	13. NUMBER OF PAGES 35	
14. MONITORING AGENCY NAME & ADDRESS (if different from Controlling Office)	15. SECURITY CLASS. (of this report) UNCLASSIFIED	
	15a. DECLASSIFICATION/DOWNGRADING SCHEDULE	
16. DISTRIBUTION STATEMENT (of this Report) Approved for public release; distribution is unlimited.		
17. DISTRIBUTION STATEMENT (of the abstract entered in Block 20, if different from Report)		
18. SUPPLEMENTARY NOTES Submitted to <u>J. Geophys. Res.</u>		
19. KEY WORDS (Continue on reverse side if necessary and identify by block number) Dynamics Explorer Field-aligned currents Auroral current sheets Current density		
20. ABSTRACT (Continue on reverse side if necessary and identify by block number) (See following page)		

DD FORM 1473
1 JAN 73EDITION OF 1 NOV 65 IS OBSOLETE
S/N 0102-LF-014-6601

UNCLASSIFIED

SECURITY CLASSIFICATION OF THIS PAGE (When Data Entered)

ABSTRACT

The current-voltage relation within narrow auroral current sheets is examined through the use of high-resolution data from the high altitude Dynamics Explorer 1 satellite. The north-south perpendicular electric field and the east-west magnetic field are shown for three cases in which there are large amplitude, oppositely directed paired electric fields and narrow current sheets. These data are shown to indicate that there is a linear "Ohm's law" relationship between the current density and the parallel potential drop within the narrow current sheets. This linear relationship had previously been verified for large-scale auroral formations greater than 20 km wide at the ionosphere. The evidence shown here extends our knowledge down to the scale size of discrete auroral arcs.

different altitudes on auroral field lines. The currents were inferred from magnetic field measurements. Parallel field line conductances of the order of 10^{-8} mho/m² were measured.

Discussions on the theory of the auroral current-voltage relationship can be found in papers by Knight [1973], Fridman and Lemaire [1980], Lyons [1980, 1981], Chiu and Cornwall [1980], Chiu et al. [1981], and Stern [1981]. In general, expressions for the upward field-aligned current density due to electrons precipitating into the ionosphere are derived from calculations of free particle motion in a dipole magnetic field. The presence of a parallel electric field above the point where the magnetospheric electrons would normally be reflected by the magnetic mirror force causes a fraction of the electrons to be precipitated. While the exact expression relating current to potential drop is fairly complex, with some assumptions the relationship can be simplified to one showing that the current density is linearly proportional to the field-aligned potential drop. The "conductance" value depends on the density and thermal energy of the magnetospheric electrons and can be expressed as [Lyons, 1981]:

$$G = \frac{e^2 n}{(2m_e K_{th})^{1/2}} = 1.07 \cdot 10^{-23} \frac{n}{K_{th}^{1/2}} \frac{J}{m^2 s V^2} \quad (1a)$$

in MKS units (this has the dimensions of mho/m²). With density given in units of cm⁻³ and energy in eV the equivalent expression is:

$$G = 2.7 \cdot 10^{-8} \frac{n}{K_{th}^{1/2}} \frac{\text{mho}}{m^2} . \quad (1b)$$

(In many papers the conductivity is referred to as K or the Lyons-Evans-Lundin constant.) With $n=1 \text{ cm}^{-3}$ and $K_{th}=250 \text{ eV}$ the conductance is $1.7 \cdot 10^{-9} \text{ mho/m}^2$. For $n=5 \text{ cm}^{-3}$ and $K_{th}=100 \text{ eV}$ the conductance is $1.4 \cdot 10^{-8} \text{ mho/m}^2$, so there appears to be a good theoretical justification for the aforementioned observations. However, there has been very little work done in the area of downward current regions, although Stern [1981] does include some discussion on this subject.

The origin of the parallel electric fields is a puzzle which remains to be solved; an assumed potential drop is used as an input to the kinetic theory. Among the mechanisms which have been suggested for producing the parallel electric fields are anomalous resistivity [Papadopoulos, 1977; Falthammar, 1977; Hudson et al., 1978; Lysak and Hudson, 1979; Lysak and Dum, 1983], double layers [Block, 1978; Goertz, 1979], and the magnetic mirror effect [Persson, 1966; Alfven and Falthammer, 1963; Lemaire and Scherer, 1974]. General discussions on the subject of parallel electric fields can be found in the reviews by Shawhan et al. [1978], Mozer et al. [1980], and Stern [1983].

There appears to be a link between parallel electric fields and the small-scale regions of very large perpendicular electric fields which were observed by Mozer et al. [1977]. There is evidence that these "electrostatic shocks," which were measured with the S3-3 satellite, are associated with discrete auroral arcs [Torbert and Mozer, 1978] and

regions of upward/downward ion/electron acceleration [Mozer et al., 1980; Temerin et al., 1981].

The question has remained: what kind of current-voltage relation is there in these narrow regions (under 20 km wide at the ionosphere) where large magnitude electric fields are found? The S3-3 satellite lacked a magnetic field measurement with sufficient spatial resolution to determine the current structure on the same size scale as the electric field [Mozer et al., 1980]. The study by Weimer et al. [1985] had been limited to structures with spatial widths greater than 20 km at the base of the field lines. This 20 km limit had been imposed by the measurement of the electric field on the high altitude DE-1 satellite, as the electric field in the spacecraft's orbit plane is measured with just one rotating double-probe. A static electric field appears in the "raw" data as a sine wave with a six second period. The electric fields which had been used in the 1985 paper had been derived from a least square error fit of the signal to a sine wave. This fitting process works extremely well for measuring the large-scale electric fields which change on a time scale greater than the satellite spin period. But the rapid, small-scale variations, which usually have the largest magnitudes, are filtered out by this process. In order to obtain the electric field with a better spatial resolution, the sine wave modulation can be removed from the data in a more direct manner. In this paper we will show DE-1 electric field measurements with the highest possible resolution, and we will compare these electric fields to magnetic field measurements with the same time (spatial) resolution. The data show that an "Ohm's law" is valid for current structures just a few km across.

II. THEORY

First we will discuss what sort of relationship is to be expected (assuming an "Ohm's law") between the north-south, perpendicular electric field and the east-west magnetic field variations. It is well known that just above the ionosphere, below the altitude of field-aligned electric fields, the height-integrated ionospheric Pedersen conductivity (Σ_p) is an important factor in the relationship between the field-aligned currents and the perpendicular electric fields. Smiddy et al. [1980] have shown that at the top of the ionosphere:

$$j_{\parallel} = - \frac{\partial E_x}{\partial x} \Sigma_p . \quad (2)$$

Here we use a coordinate system in which the Z axis is upward along the magnetic field line, X is southward, and Y is eastward. This quantity j_{\parallel} is the magnetic field-aligned current density, which can be inferred from the derivative of the east-west magnetic field component measured on a satellite which is moving in the north-south direction. The currents are assumed to be in the form of "infinite sheets," i.e., much larger in the east-west and up-down directions than their width in the north-south direction. With this assumption, the magnetic and electric fields are related to each other according to

$$\Delta B_y = -\mu_0 \Sigma_p E_x \quad (3)$$

where ΔB_y is the difference between the measured magnetic field and the earth's dipole field. Equation (3) has been confirmed by a number of measurements of magnetic and electric fields just above the ionosphere [Smiddy et al. 1980; Sugiura, 1984]. At higher altitudes Equation (3) may not be valid due to the possible existence of an electric potential drop parallel to the magnetic field (V_{\parallel}). The "Ohm's law" we are investigating assumes that the field-aligned current density at the ionosphere and the parallel potential drop are related by

$$j_{\parallel} = -GV_{\parallel} \quad (4)$$

where G is the field line conductance. The sign convention is such that the current is positive (upward) when the potential decreases in going from low to high altitude, so that the potential drop, $V_{\parallel} = V_{\text{high}} - V_{\text{low}}$, is negative.

It is shown by Weimer et al. [1985] that with the definition of a constant inverse scale length or "critical wavenumber,"

$$\frac{G}{\Sigma_p} \equiv k_o^2 \quad (5)$$

the Fourier transforms of the high-altitude quantities j_{\parallel} , B_y , and E_x have a relationship which depends on their spatial wavenumber, k :

$$\tilde{j} = \frac{-i k}{(k/k_0)^2 + 1} \Sigma_P \tilde{E}_x \quad (6)$$

$$\mu_0 \tilde{j}_{\parallel} = i k \tilde{B}_y \quad (7)$$

The tildas indicate that the quantities are transformed from a spatial domain to a wavenumber domain. The spatial variations are presumed to be in the north-south (x) direction.

With a field line conductance of 10^{-8} mho/m² and a Pedersen conductance of 5 to 10 mho, the inverse of the critical wavenumber, k_0^{-1} , will be in the range of 22 to 32 km. The wavelength $\lambda_0 = 2\pi/k_0$ is 140 to 200 km. At the limit of a very small wavelength and large wavenumber, where $(k/k_0)^2 \gg 1$, Equation (6) can be simplified to

$$\tilde{j} = -(i/k)G \tilde{E}_x \quad (8)$$

From Equation (4) we see that

$$-ik\tilde{V}_{\parallel} = \tilde{E}_x \quad (9a)$$

or in real space,

$$-\frac{\partial V_{\parallel}}{\partial x} = E_x \quad (9b)$$

where E_x is the measured electric field at the satellite altitude. Therefore, at very small wavelengths the ionospheric conductivity does not influence the high altitude electric field, and there is a very simple relationship between the north-south electric field and the parallel potential drop. By integrating E_x one can obtain a "potential profile" (V_{\parallel} as a function of x), which should be proportional to the current density if the "Ohm's law" of Equation (4) is correct. Integration of E_x a second time (with multiplication by 'a' and μ_0) should result in ΔB_y . This prediction can be tested by comparing E_x and ΔB_y in cases where the short wavelength variations are large in comparison to the long wavelength variations.

III. OBSERVATIONS

The electric field in the orbit plane of the DE-1 satellite is measured with a double-probe antenna measuring 200 m tip-to-tip. The electric field is sampled at a rate of 16 samples per second by the Plasma Wave Instrument. The complete instrument description is given by Shawhan et al. [1981]. The "raw" electric field is modulated by the satellite's rotation, which has a six second period. With the assumption that the electric field is perpendicular to the magnetic field, the spin modulation can be removed by dividing each measurement by the sine of the angle between the double-probe antenna and the magnetic field in the spin plane. This demodulation procedure works well when the "spin phase angle" is large, but when the antenna is nearly parallel to the magnetic field there can be problems: a small error in the phase angle results in a distorted electric field, which goes to infinity when the angle is zero. To eliminate this effect gaps are introduced in the de-spin data whenever the magnitude of the phase angle is less than 30 degrees.

The top panel in Figure 1 shows 30 seconds of high resolution electric field data which has had the spin modulation removed by this technique. As subsequent steps in the data analysis require a continuous electric field, the gaps have been filled in with values which smoothly connect the data on both sides of the gaps. The time axis on the plot has been marked with shaded blocks to indicate where

these gaps occur. The resulting graph shows a large amplitude electric field which points southward for 6.0 seconds then reverses to a northward direction for 3.5 seconds. At the time of this measurement the velocity component of DE-1 perpendicular to the magnetic field was 4.77 km/sec in a southward direction, therefore the total width of this structure is 45 km. The satellite was located at an altitude of 10,500 km and invariant latitude of 69.4° , so the 45 km maps to a width of 9.5 km at the base of the magnetic field line.

Integration of the electric field in Figure 1 results in the electric potential function which is shown in the second plot from the top in the same figure. The integration is done by adding each data point to a sum, after multiplication by the appropriate time and velocity constants. Multiplication of the potential by a conductance results in a value for the local current density; the integration of this current density, equivalent to the second integral of the electric field, results in the east-west deviation of the magnetic field shown in the third plot. The bottom plot in Figure 1 shows the actual value of the east-west magnetic field measured with the magnetometer on DE-1 [Farthing et al., 1981]. This magnetic field, which is also sampled at 16 data points per second, has had the background field due to the earth's dipole subtracted and has been filtered to remove high frequency noise.

Figure 1 shows a very good match between the second integral of the electric field and the measured magnetic field. To obtain such a good agreement, a trial-and-error adjustment of two parameters was necessary. These parameters are an offset potential and the field-line

conductance. The potential in Figure 1 is shown to start at zero; a constant voltage may be added to compensate for the actual initial value. An offset of +200 volts, added before the second integration, yielded the best match with the magnetic field. This positive potential at the high altitude location should correspond to a downward current. Figure 2, which shows the measured east-west magnetic field for a longer time interval, indicates that the addition of a positive potential is justified. Prior to the electric field spike at 3:45:25 UT there was a gradual negative (westward) slope in the magnetic field, which corresponds to a downward current. The large electric fields are located on the boundary between this downward current and a broad upward current region. A narrow but large magnitude upward current sheet is located right on the boundary. This peak in the upward current occurs precisely at the point where the high altitude potential is most negative.

The addition of a constant to the potential is equivalent to adding a constant slope to the second integral (model magnetic field). The magnitudes of the relative changes in the magnetic field are determined by the value chosen for the field line conductance. In this case a conductance of $4 \cdot 10^{-10}$ mho/m² yielded the best match between the model and measured magnetic field. At the point where the potential drop is -1300 volts the local current density is $5.2 \cdot 10^{-7}$ A/m². Due to the convergence of the magnetic flux tubes, both the current density and the east-west magnetic field increase towards lower altitudes. The "mapping" factor for both of these quantities from a high altitude location to the base of the magnetic field line is $L^{3/2} \cos^3 \lambda_m$, where

λ_m is the magnetic latitude. For this case the mapping factor is 4.32, so the "normalized" field line conductance is $1.7 \cdot 10^{-9}$ mho/m². This is the ratio between the current density at the base of the field line ($2.2 \cdot 10^{-6}$ A/m²) and the total potential drop along the field line (1.3 kV). However, if there is an additional potential drop above the satellite, then this measurement of the total potential is too low, and the estimate for the conductivity is too high.

For this case from October 19 (day 292), 1981, it is instructive to examine the data from the High Altitude Plasma Instrument (HAPI) on DE-1. The instrument description is in the paper by Burch et al. [1981]. In Figure 3 are shown a sequence of electron and ion distribution functions measured with the HAPI from 3:45:12 to 3:45:48 UT. Each distribution function is derived from data collected by the instrument during two complete rotations of the spacecraft. There are very distinct changes in the distribution functions as the spacecraft moves across the region with the large electric fields. Initially the distribution functions are rather symmetrical; after crossing the region where the high altitude potential goes from positive to negative, there is evidence of ions which have been accelerated up the field lines and a wide electron loss cone, indicative of a parallel electric field below the spacecraft. There are only low energy (160 eV) electron "beams" going down the field lines, indicating that there is not a significant parallel potential drop above the satellite. These changes in the distribution functions were coincident with the entry of DE-1 into the boundary plasma sheet (the sudden increase in electron temperature is more obvious in a color energy-time spectrogram of the electron distribution function, not shown here).

There are indications of ions moving upward with the energies predicted by the electric potential, such as the contour "island" at $V_{\parallel} = -470$ km/sec (1200 eV) from 3:45:24.6 to 3:45:36.6 UT. However, a greater number of ions appear to have been accelerated to higher energies--up to 3 keV. This puzzle is perhaps related to the observations by Mizera et al. [1981] and Collin et al. [1981] of O^+ ions being more energetic than the H^+ ions. The distribution functions shown in Figure 3 are for all ions, as the energies are measured without a distinction between species. On the other hand, the electron loss cones appear to be in better agreement with the potential drop obtained from the electric field. The very wide loss cone from 3:45:24.6 to 3:45:36.6 UT corresponds to a potential drop of about 1400 volts; in the distribution function for the next time interval the loss cone is more narrow, corresponding to about 600 volts. These are only ballpark figures, as the loss cone calculation depends on the altitude at which the parallel electric field is assumed to be located.

Another case for study is shown in Figure 4. The data is from October 23 (Day 296), 1981. The format is the same as in Figure 1. This event has some similarities to the previous case, yet there are important differences. Figure 5 shows that, like before, the electric field "spike" occurred on the southward edge of a region of downward current. But this time the downward current is much larger in magnitude and confined to a relatively narrow region, embedded within a larger region of upward current (Lin et al. [1985] show large-scale "inverted-V" regions on both sides of this same event in their Plate 1). Whereas in the previous case most of the magnetic field variations were due to

upward currents, in this second example the downward currents are equally important.

As before, different parameters were tested in order to find a model magnetic field which best matched the measured field. In this case the most reasonable results were obtained with the addition of a +3 mV/m offset to the electric field before doing the first integration. This compensated for a negative (northward), large-scale convection electric field which would be linearly proportional to ΔB according to Equation 3. A +500 volt offset was added to the potential before doing the second integration. This is justifiable on the basis that the region of downward current had been penetrated a few seconds before the starting time of Figure 4. A conductance of $4 \cdot 10^{-10}$ mho/m² was used to generate the model magnetic field. The DE-1 satellite was at an altitude of 9000 km and an invariant latitude of 65.1°, so the current projection factor to the field line base is 3.75. This results in a normalized field line conductance of $1.5 \cdot 10^{-9}$ mho/m².

The final example is shown in Figure 6, from October 30 (day 303), 1981. In this case the match between the second integral of the electric field and the measured magnetic field is not as good as in the previous examples. A potential offset of +200 volts and a conductance of $4 \cdot 10^{-10}$ mho/m² were used to generate the second integral shown in Figure 6. Figure 7 shows that, just like the previous cases, the large perpendicular electric fields are located on the edges of a narrow but very intense current sheet which is located on a boundary between large-scale downward and upward currents. The main difference between this and the previous cases is that the magnitudes are greater: the

electric field reaches 320 mV/m, the potential exceeds 3 kV, and the current density is greater than $1.2 \cdot 10^{-6}$ A/m² (the ionospheric current density is 5.12 times higher). The "model" magnetic field is very much similar to the measured field up to 13:11 UT, after which the measured field levels off and the integrated value continues to increase. A higher conductance of $7 \cdot 10^{-10}$ mho/m² (with a normalized value of $3.6 \cdot 10^{-9}$ mho/m²) makes a better match for the period up to 13:11 UT, but after that point a higher conductance makes the disagreement worse. The problem may be due to inaccurate electric fields in the data gaps.

IV. DISCUSSION AND SUMMARY

The evidence which has been shown here provides a convincing case for the validity of Equation 4 within current sheets with small spatial widths. The linear relationship between current density and potential is the simplest and, as far as we know, only explanation for the magnetic field signatures which are observed concurrent with the large amplitude electric fields. In general, the large amplitude perpendicular electric fields occur on the boundary between upward and downward currents, where the high altitude potential must reverse signs within a short distance. The potential difference between the magnetosphere and ionosphere needs to change signs in order that the currents flow in the direction from high to low potential.

The changes in the ionospheric potential, due to the convection electric field, are a very important factor in the large-scale pattern of field-aligned currents. In general it would not be possible to make a determination of the field-aligned potential drop based on just a measurement of the high altitude electric field. However, we have shown here that within current sheets with very small "wavelengths" the ionospheric potential may be treated as a constant.

A theory based on a linear "Ohm's law" shows that for the small-scale features the second integral of the north-south electric field should be proportional to the east-west magnetic field variations. The data which have been shown here support this theory. In order to show

the good agreements between the second integral of the measured electric field and the measured magnetic field it was necessary to adjust two unknown quantities--the potential offset and the field-aligned conductance. These adjustments were within reason and relatively minor. The second integral would not have given the observed agreement if the "Ohm's law" was not a good approximation. Indeed, given the gaps in the electric field data it is amazing that the integrated values come as close as they do to matching the measured magnetic fields, since the integrations cause errors to accumulate forward in time.

The normalized field line conductances determined with this technique generally are close to 10^{-9} mho/m². The question remains: which of the proposed mechanisms for creating a parallel potential drop along magnetic field lines can account for a conductance of this value? This conductance is within the limits of the kinetic theory (Equation 1), although Fridman and Lemaire [1980] predict values which are smaller by a factor of 10. Evidence in favor of the magnetic mirror effect (hot electrons and ions mirror at different points on field lines, causing charge separation) as the source of a parallel potential drop is found in the first case shown here, as the potential jumped suddenly when DE-1 entered the plasma boundary sheet. However, the kinetic theory works in one direction only--for upward currents due to downward precipitating electrons. In the second example we have shown (Figure 4) the conductance is the same for both upward and downward currents. In every case short wavelength "turbulence" in the electric field is present where the currents are most intense, suggesting that large amplitude plasma waves may be present. Anomalous resistivity may be important.

Wave particle interactions might also explain how some ions get accelerated to energies higher than the measured potential drop.

From these data it is not possible to tell how the potential drop is distributed along the field lines. Abrupt jumps in the form of double layers may well be present. Our results are consistent with the stationary V-shaped and S-shaped electric equipotential models which are shown in the papers by Hudson and Mozer [1978] and Mozer et al. [1980]. Figures 1 and 6 are good examples of cases where S-shaped contours are present. These appear to be the most common. The potential contour for the case in Figure 4 would be more like a V-shape, but inverted from the usual convention as it is associated with downward instead of upward current.

Finally, we address the "chicken and egg" problem of the origin of the field-aligned currents and potential drops. This is equivalent to asking if the source is a current or voltage generator. On the very large scale it is likely that the current systems are driven by voltage generators. However, Lysak [1985] has shown that small-scale structures are more consistent with current generators. The data shown here suggest that this is the case. The Kelvin Helmholtz instability may be the source of these small-scale currents (P. F. Bythrow, unpublished manuscript, 1985). The currents would then produce the parallel potential drops, perhaps by anomalous resistivity and/or the formation of double layers. We note that the "Ohm's law" also implies that $\bar{\mathbf{j}} \cdot \bar{\mathbf{E}} > 0$ above the ionosphere and that electromagnetic energy is dissipated through ion/electron acceleration in the magnetosphere.

ACKNOWLEDGEMENTS

The research at the University of Iowa was supported by NASA through grants NAG5-310, NGL-16-001-002 and NGL-16-001-043, and by the Office of Naval Research through contract N00014-85-K-0183. The research at Southwest Research Institute was supported by NASA through contract NAS5-28711. The research at Regis College was supported by U.S. Air Force contract F19628-84-C-0126.

REFERENCES

- Alven, H. and C.-G. Falthammar, Cosmical Electrodynamics, 2nd ed., Oxford University Press, New York, 1963.
- Block, L. P., A double layer review, Astrophys. Space Sci., 55, 59, 1978.
- Burch, J. L., J. D. Winningham, V. A. Blevins, N. Eaker, W. C. Gibson, and R. A. Hoffman, High-altitude plasma instrument for Dynamics Explorer-A, Space Sci. Instrum., 5, 455, 1981.
- Chiu, Y. T. and J. M. Cornwall, Electrostatic model of a quiet auroral arc, J. Geophys. Res., 85, 543, 1980.
- Chiu, Y. T., A. L. Newman, and J. M. Cornwall, On the structure and mapping of auroral electrostatic potentials, J. Geophys. Res., 86, 10,029, 1981.
- Collin, H. L., R. D. Sharp, E. G. Shelley, and R. G. Johnson, Some general characteristics of upflowing ion beams over the auroral zone and their relationship to auroral electrons, J. Geophys. Res., 86, 6820, 1981.
- Falthammar, C.-G., Problems related to macroscopic electric fields in the magnetosphere, Rev. Geophys. and Space Phys., 15, 457, 1977.
- Farthing, W. H., M. Sugiura, B. G. Ledley, and L. J. Cahill, Magnetic field observations on DE-A and -B, Space Sci. Instrum., 5, 551, 1981.

- Fridman, M. and J. Lemaire, Relationship between auroral electron fluxes and field aligned electric potential differences, J. Geophys. Res., 85, 664, 1980.
- Goertz, C. K., Double layers and electrostatic shocks in space, Rev. Geophys. and Space Phys., 17, 418, 1979.
- Hudson, M. K., R. L. Lysak, and F. S. Mozer, Magnetic field-aligned potential drops due to electrostatic ion cyclotron turbulence, Geophys. Res. Lett., 5, 143, 1978.
- Hudson, M. K. and F. S. Mozer, Electrostatic shocks, double layers, and anomalous resistivity in the magnetosphere, Geophys. Res. Lett., 5, 131, 1978.
- Knight, S., Parallel electric fields, Planet. Space Sci., 21, 741, 1973.
- Lemaire, J. and M. Scherer, Ionosphere-plasmasheet field-aligned currents and parallel electric fields, Planet. Space Sci., 22, 1485, 1974.
- Lin, C. S., J. N. Barfield, J. L. Burch, and J. D. Winningham, Near-conjugate observations of inverted-V electron precipitation using DE 1 and DE 2, J. Geophys. Res., 90, 1669, 1985.
- Lyons, L. R., D. S. Evans, and R. Lundin, An observed relation between magnetic field-aligned electric fields and downward electron energy fluxes in the vicinity of auroral forms, J. Geophys. Res., 84, 457, 1979.

- Lyons, L. R., Generation of large-scale regions of auroral currents, electric potentials, and precipitation by divergence of the convection electric fields, J. Geophys. Res., 85, 17, 1980.
- Lyons, L. R., Discrete aurora as the direct result of an inferred high-altitude generating potential distribution, J. Geophys. Res., 86, 1, 1981.
- Lysak, R. L. and M. K. Hudson, Coherent Anomalous Resistivity in the region of electrostatic shocks, Geophys. Res. Lett., 6, 661, 1979.
- Lysak, R. L. and C. T. Dum, Dynamics of magnetosphere-ionosphere coupling including turbulent transport, J. Geophys. Res., 88, 365, 1983.
- Lysak, R. L., Auroral electrodynamics with current and voltage generators, J. Geophys. Res., 90, 4178, 1985.
- Menietti, J. D., and J. L. Burch, A satellite investigation of energy flux and inferred potential drop in auroral electron energy spectra, Geophys. Res. Lett., 8, 1095, 1981.
- Mizera, P. F., J. F. Fennell, D. R. Croley, A. L. Vampola, F. S. Mozer, R. B. Torbert, M. Temerin, R. Lysak, M. Hudson, C. A. Cattell, R. L. Johnson, R. D. Sharp, A. Ghielmetti, and P. M. Kintner, The aurora inferred from S3-3 particles and fields, J. Geophys. Res., 86, 2329, 1981.
- Mozer, F. S., C. W. Carlson, M. K. Hudson, R. B. Torbert, B. Parady, and J. Yatteau, Observations of paired electrostatic shocks in the polar magnetosphere, Phys. Rev. Lett., 38, 292, 1977.

- Mozer, F. S., C. A. Cattell, M. K. Hudson, R. L. Lysak, M. Temerin, and R. B. Torbert, Satellite measurements and theories of low altitude auroral particle acceleration, Space Sci. Rev., 27, 155, 1980.
- Papadopoulos, K., A review of anomalous resistivity for the ionosphere, Rev. Geophys. and Space Phys., 15, 113, 1977.
- Persson, H., Electric fields parallel to the magnetic field in a low-density plasma, Phys. Fluids, 9, 1090, 1966.
- Shawhan, S. D., C.-G. Falthammer, and L. P. Block, On the nature of large auroral zone electric fields at $1-R_E$ altitude, J. Geophys. Res., 83, 1049, 1978.
- Shawhan, S. D., D. A. Gurnett, D. A. Odem, R. A. Helliwell, and C. G. Park, The plasma wave instrument and quasi-static electric field instrument (PWI) for Dynamics Explorer-A, Space Sci. Instrum., 5, 535, 1981.
- Smiddy, M., W. J. Burke, M. C. Kelley, N. A. Saflekos, M. S. Gussenhoven, D. A. Hardy, and F. J. Rich, Effects of high-latitude conductivity on observed convection electric fields and Birkeland currents, J. Geophys. Res., 85, 6811, 1980.
- Stern, D. P., One-dimensional models of quasi-neutral parallel electric fields, J. Geophys. Res., 81, 5839, 1981.
- Stern, D. P., Electric currents and voltage drops along auroral field lines, Space Sci. Rev., 34, 317, 1983.
- Sugiura, M., A fundamental magnetosphere-ionosphere coupling mode involving field-aligned currents as deduced from DE-2 observations, Geophys. Res. Lett., 11, 9, 877, 1984.

Temerin, M., C. Cattell, R. Lysak, M. Hudson, R. B. Torbert, F. S.

Mozer, R. D. Sharp, and P. M. Kintner, The small-scale structure of electrostatic shocks, J. Geophys. Res., 86, 11278, 1981.

Torbert, R. B. and F. S. Mozer, Electrostatic shocks as the source of discrete auroral arcs, Geophys. Res. Lett., 5, 135, 1978.

Weimer, D. R., C. K. Goertz, D. A. Gurnett, N. C. Maynard, and J. L. Burch, Auroral zone electric fields from DE-1 and -2 at magnetic conjunctions, J. Geophys. Res., 90, 7479, 1985.

FIGURE CAPTIONS

- Figure 1 Electric and magnetic fields measured with DE-1 in the 30 second interval from 3:45:15 to 3:45:45 UT on October 19 (day 292), 1981. The top graph is the north-south electric field measured in the orbit plane. The data has had the spin modulation removed; the blocks above the time axis indicate where "gaps" have been filled in. The second graph shows the potential obtained by integrating this electric field, and the third graph shows a model of the east-west magnetic field obtained by a second integration. At the bottom is shown the measured magnetic field. A positive slope is indicative of passage through an upward current. The DE-1 spacecraft was moving north to south in the northern hemisphere at this time.
- Figure 2 East-west magnetic field component from the magnetometer on DE-1 for the time period from 3:43 to 3:49 UT on October 19 (day 292), 1981. The earth's dipole field has been subtracted from the measured values.
- Figure 3 Phase-space contours of the logarithm of the electron and ion distribution functions measured by DE-1 from 3:45:12.5 to 3:45:36.7 UT on October 19 (day 292), 1981. Each 12 second segment spans two spacecraft spin periods. The ion energies were measured with no distinction between species. The ion velocity scale is indicated for H^+ ions.

- Figure 4 Electric and magnetic fields measured with DE-1 in the time period from 3:45:04 to 3:45:34 UT on October 23 (day 296), 1981. The format is the same as in Figure 1.
- Figure 5 East-west magnetic field component from the magnetometer on DE-1 for the time period from 3:43 to 3:49 UT on October 23 (day 296), 1981.
- Figure 6 Electric and magnetic fields measured with DE-1 in the time period from 13:27:55 to 13:28:25 UT on October 30 (day 303), 1981. The format is the same as in Figure 1.
- Figure 7 East-west magnetic field component from the magnetometer on DE-1 for the time period from 13:25 to 13:31 UT on October 30 (day 303), 1981.

C-685-860

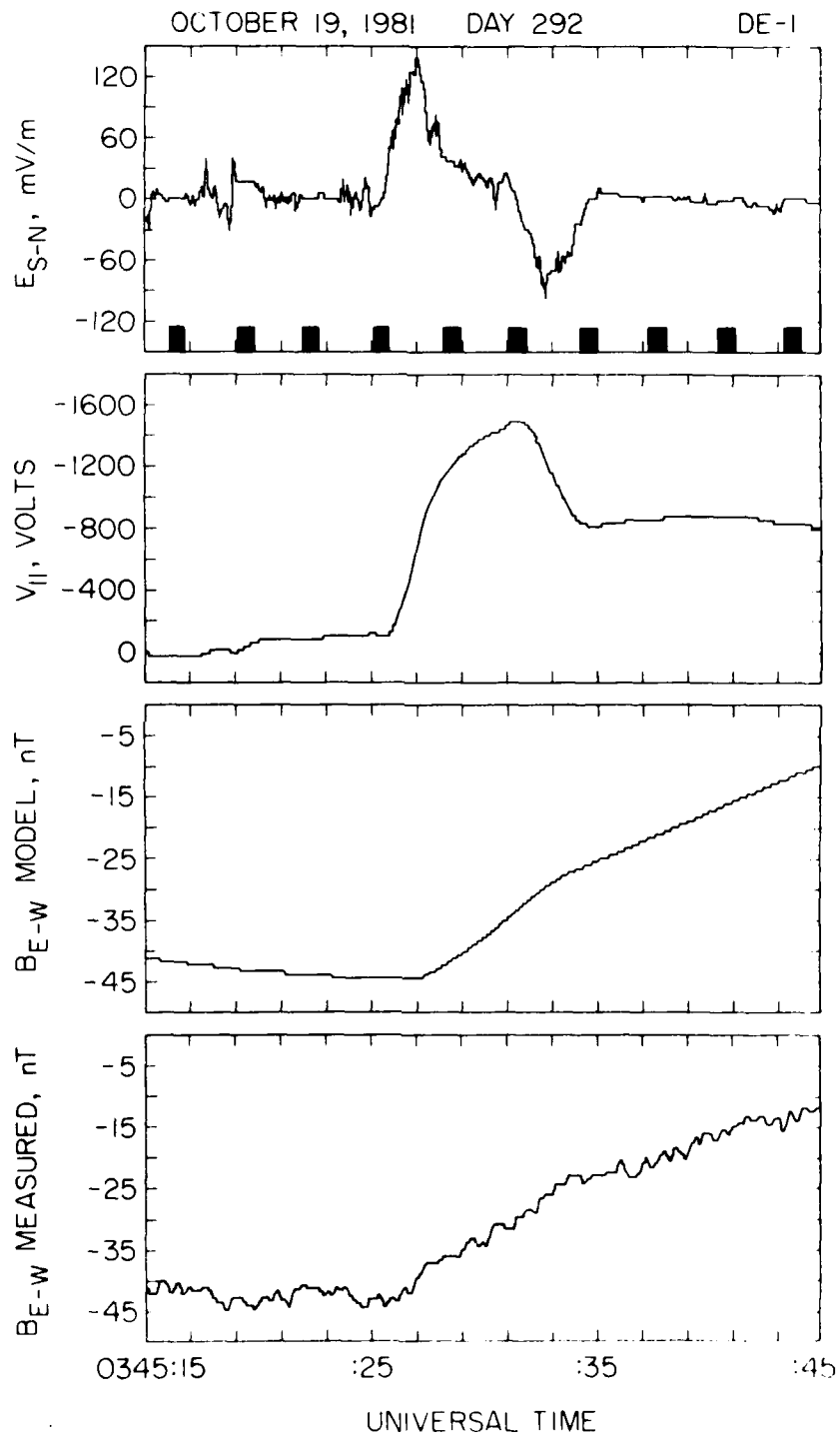
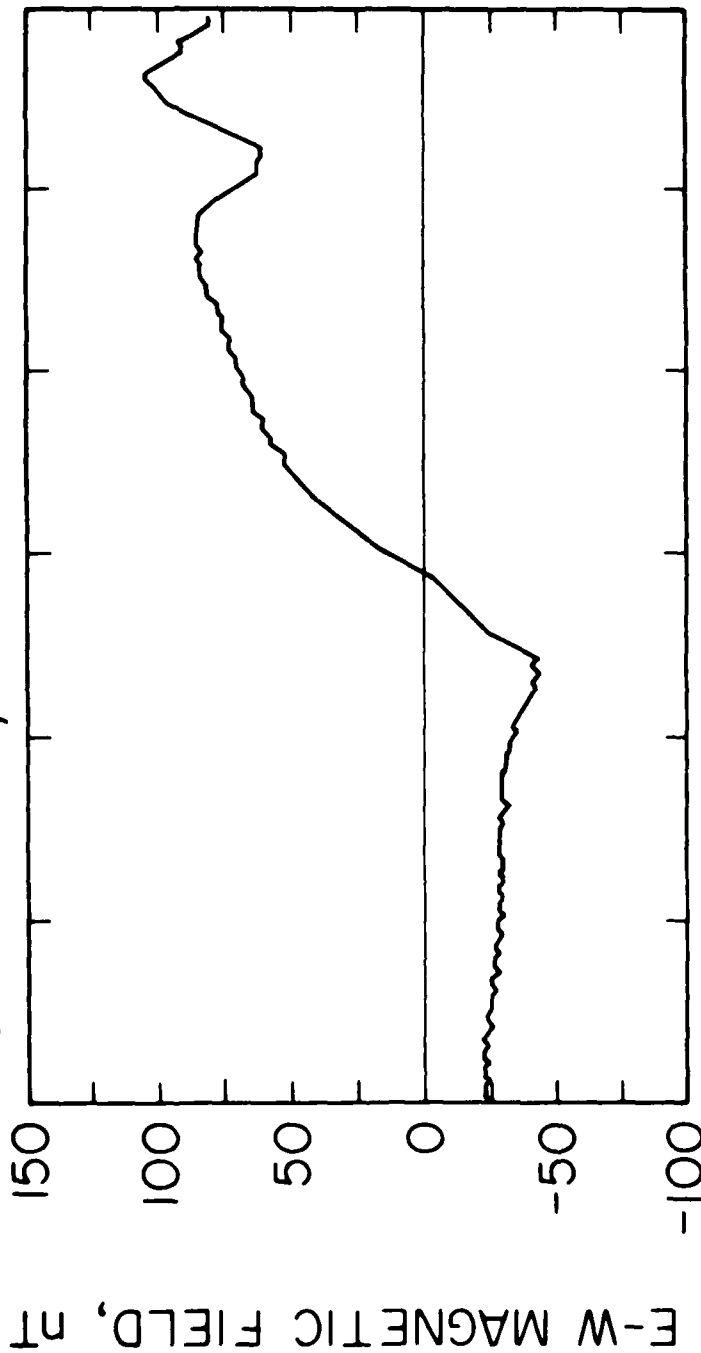


Figure 1

A-G85-857

OCTOBER 19, 1981 DAY 292 DE-1



UT 03:43 03:45 03:47 03:49

INV LAT 70.74 69.67 68.54 67.35

Figure 2

D-685-1056

DE-1 HAPI ELECTRONS OCTOBER 19, 1981 DAY 292

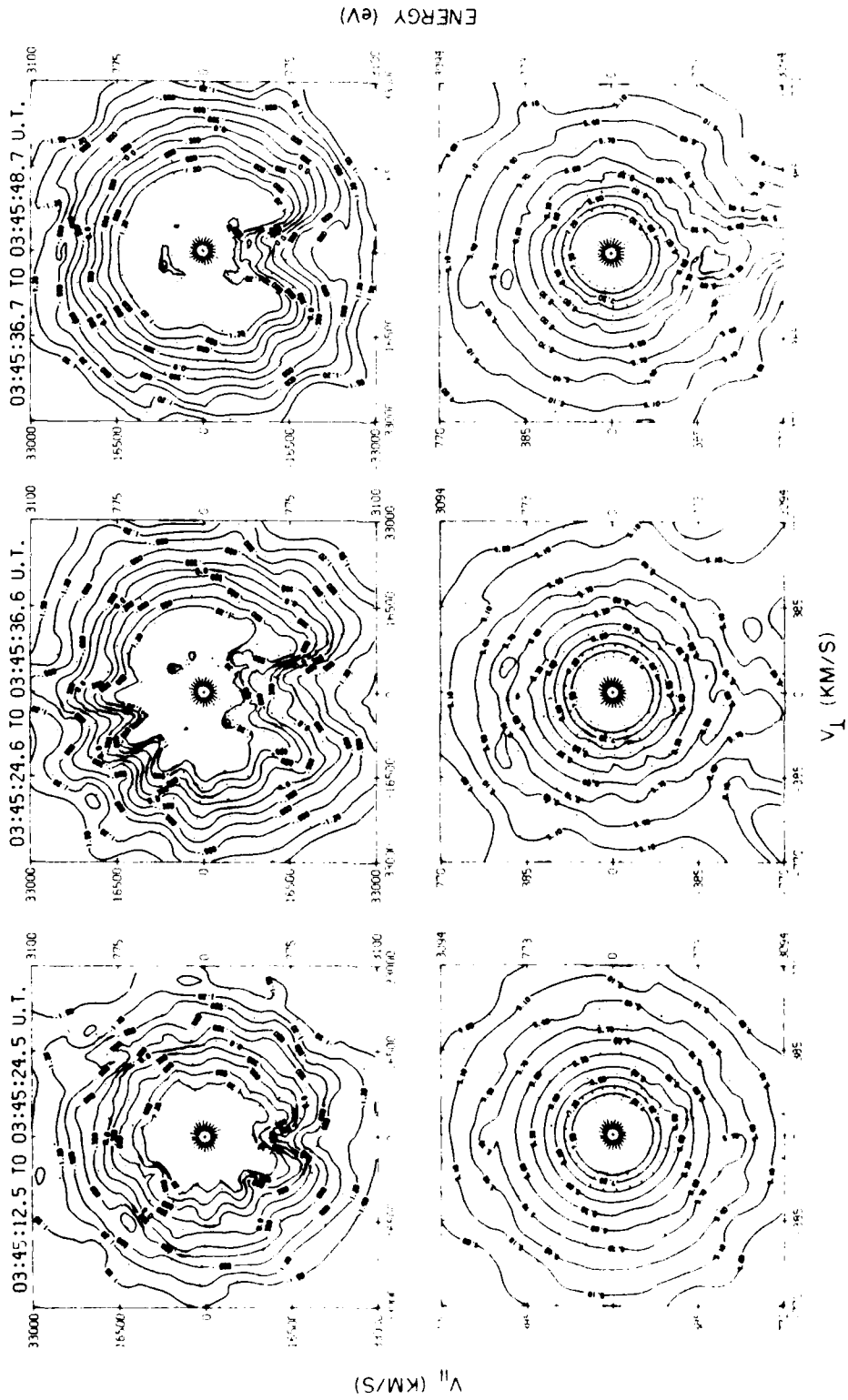


Figure 3

OCTOBER 23, 1981 DAY 296 DE-1

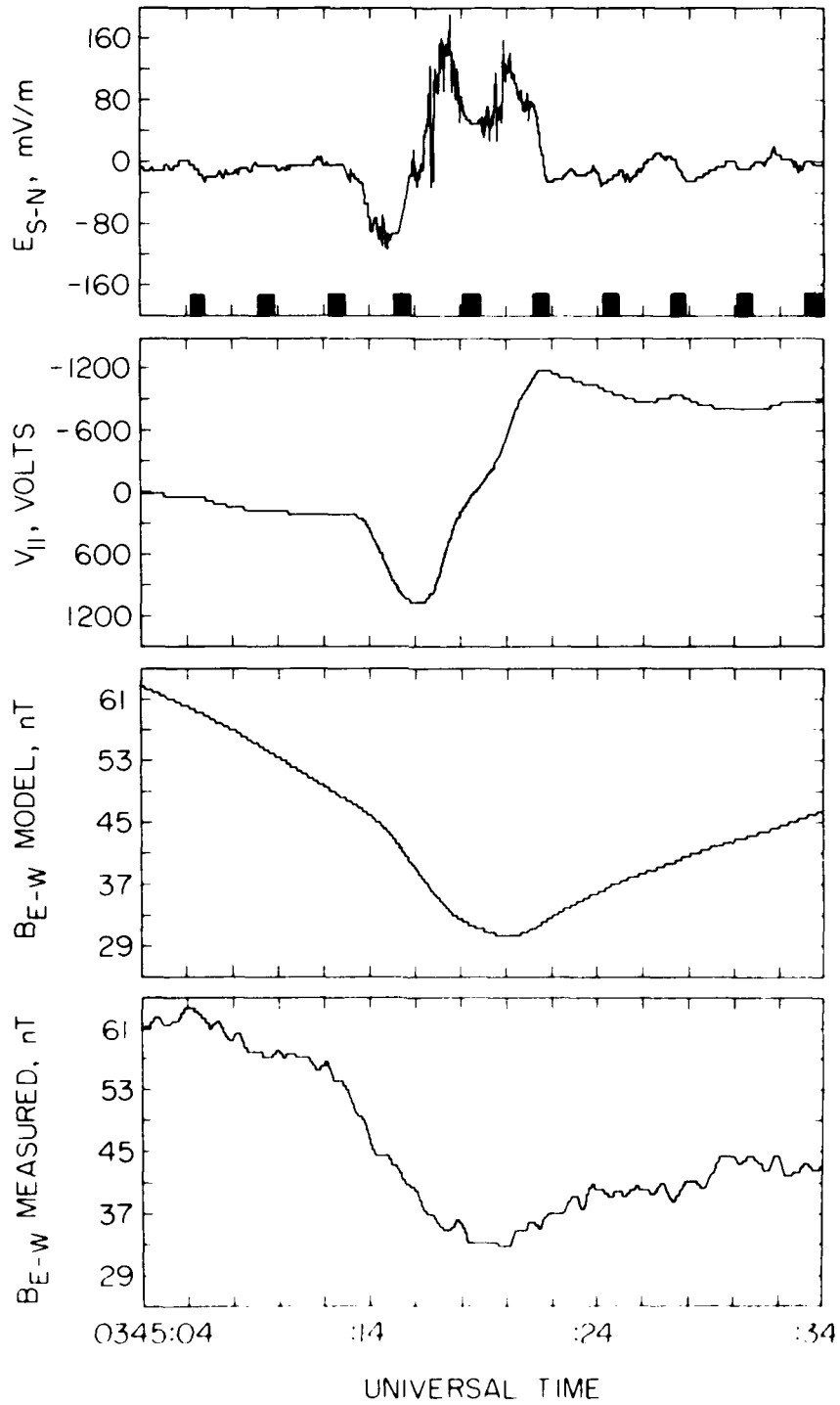
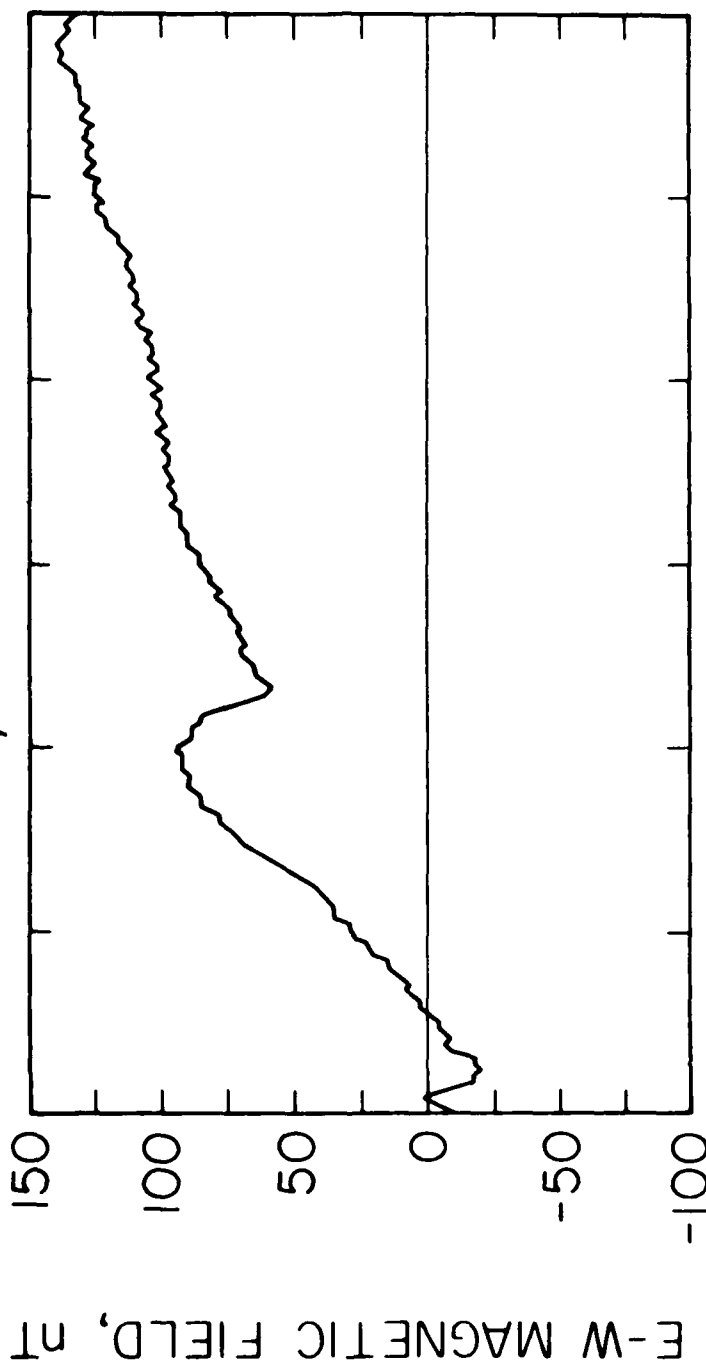


Figure 4

A-G85-856

OCTOBER 23, 1981 DAY 296 DE-1



UT 03:43 03:45 03:47 03:49
INV LAT 66.64 65.29 63.85 62.32

Figure 5

C-85 861

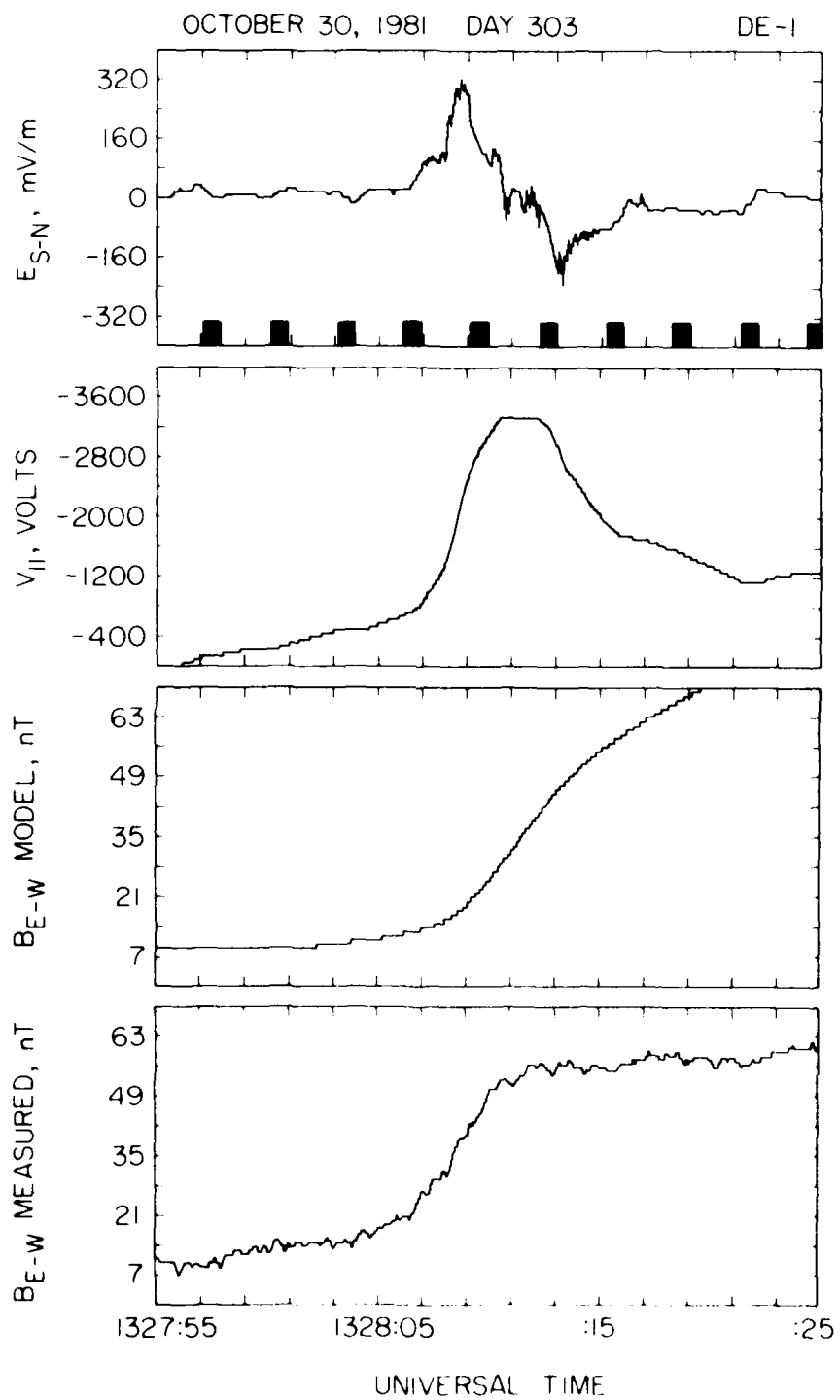
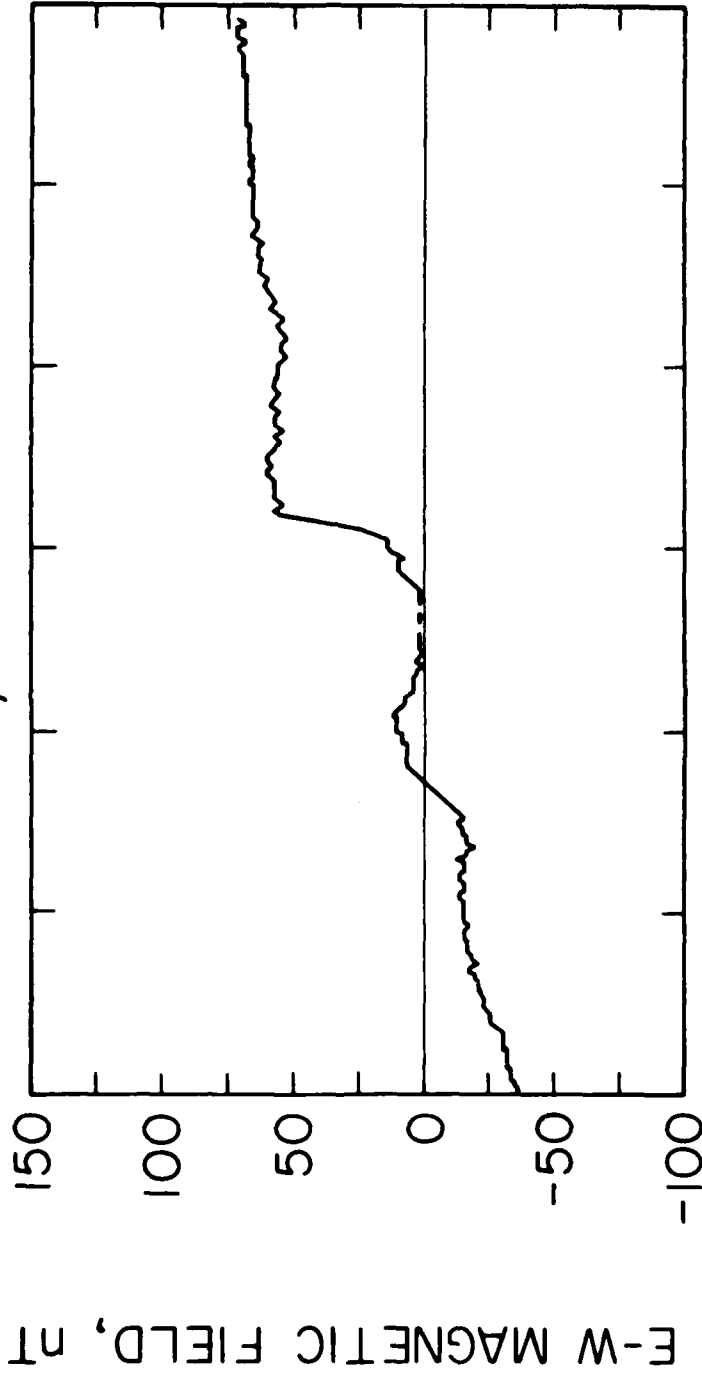


Figure 6

A-G85-858

OCTOBER 30, 1981 DAY 303 DE-1



UT 13:25 13:27 13:29 13:31
INV LAT 68.49 67.73 66.93 66.09

Figure 7

END

DTIC

7-86